Research article

Deciphering the role of PLCD3 in lung cancer: A gateway to glycolytic reprogramming via PKC-Rap1 activation

Liang Zhang [a,b,1,*], Mingjiang Li [b], Xiaoping Li [b], Ting Xiao [c], Honggang Zhou [c], Weidong Zhang [b,**], Ping Wang [a,***]

[a] Tianjin Medical University Cancer Institute & Hospital, Tianjin, PR China
[b] Department of Thoracic Surgery, Tianjin First Central Hospital, Tianjin, 300192, PR China
[c] College of Pharmacy and Key Laboratory of Molecular Drug Research, Nankai University, Tianjin, PR China

ABSTRACT

PLCD3 belongs to the phospholipase C delta group and is involved in numerous biological functions, including cell growth, programmed cell death, and specialization. However, the role of PLCD3 in lung cancer still needs further investigation. This research aimed to investigate if PLCD3 influences glycolytic reprogramming and lung cancer development through the PKC-dependent Rap1 signaling pathway. This study found that PLCD3 was increased in lung cancer tissues. PLCD3 promotes the proliferation and invasion of lung cancer cells by activating the PKC-dependent Rap1 pathway. The detailed process involves PLCD3 triggering PKC, which subsequently stimulates the Rap1 pathway, leading to glycolytic reprogramming that supplies adequate energy and metabolic substrates necessary for the growth and spread of lung cancer cells. Moreover, PLCD3 can also promote the metastasis and invasion of lung cancer cells by activating the Rap1 pathway. This study reveals the mechanism of PLCD3 in lung cancer and provides new ideas for the treatment of lung cancer. Inhibiting PLCD3, PKC, and the Rap1 pathway may be an effective strategy for treating lung cancer.

1. Introduction

Due to the swift progress of the social economy and worsening environmental pollution, lung cancer has emerged as the highest among male malignant tumors [1]. The rate of lung cancer in women has surged quickly, placing it among the top three most frequent malignant tumors in females [2]. Tumors reprogram glucose metabolism to provide themselves with materials and energy to meet their rapid growth needs [3,4]. Research indicates that different metabolic enzymes and signaling molecules related to glucose metabolism are crucial in the formation and progression of tumors, making them key targets for diagnosing and treating malignant cancers [5,6].

PLCD3 belongs to the phospholipase C delta group and is involved in numerous biological activities, including cell growth, programmed cell death, and cellular differentiation [7]. Recent research indicates that PLCD3 is also significant in cancer development

[8]. PLCD3 enhances the growth and survival of cancer cells by triggering signaling routes like the Ras and PI3K/Akt pathways [9]. PLCD3 levels are increased in multiple types of cancer, including breast, lung, and stomach cancers [8,9]. As a result, PLCD3 serves as a biomarker for identifying and managing cancer. Nonetheless, it remains unreported if PLCD3 influences the energy metabolism of cancer cells and the subsequent molecular pathways involved.

PKC (protein kinase C) is a key signaling protein that plays a crucial role in various biological processes, such as including cell growth, survival, differentiation, programmed cell death, and cytoskeletal reorganization [10]. PKC promotes tumor cell invasion and metastasis by activating signaling pathways such as the Ras pathway and the PI3K/Akt pathway [11]. Rap belongs to the Ras family and has two subtypes, Rap1 and Rap2. Rap functions as a molecular switch by binding to GTP or GDP and switching between active and inactive states. Rap1 controls many important signaling pathways in cells [12]. Cell polarity formation, proliferation, differentiation, and carcinogenesis, cell adhesion, and movement are all pathways regulated by Rap1 [13,14]. Moreover, Rap1 is crucial in the initiation and progression of cancer.

In this study, we described the role of PLCD3 in the prognosis and biological progression of lung cancer patients. By detecting cell cycle-related proteins, we found that PLCD3 deficiency can regulate the cell cycle arrest of lung cancer cells. Glucose uptake and consumption were detected to determine whether PLCD3 is a key regulatory factor in glycolysis reprogramming. We examined how PLCD3 influences the Rap1 signaling pathway and analyzed its connection with PKC. Overall, our results provide new insights into the pathological biological role of PLCD3, which helps to better understand the potential mechanism of glycolysis reprogramming in lung cancer. This study also further identifies PLCD3 as a potential therapeutic target for lung cancer.

2. Methods

2.1. Correlation analysis of PLCD3 expression level and overall survival of lung cancer patients

Correlation analysis of PLCD3 expression level and overall survival of lung cancer patients. By employing the Kaplan-Meier method, PLCD3 served as the criterion for categorizing patients into high and low expression groups, followed by an analysis of their overall survival times and the creation of survival curves.

2.2. HPA database

Human Protein Atlas (HPA) database (https://www.proteinatlas.org/) is a comprehensive human proteomics portal. This research utilized the HPA database to examine the immunohistochemical staining of PLCD3 in both lung cancer and healthy lung tissues.

2.3. GO and KEGG analysis

GO functional enrichment are sorted according to the Enrichment score, which is the P value (-log10 conversion). The KEGG database was used to identify pathways in which differentially expressed genes were enriched (http://www.kegg.jp/). The most significant pathways were selected for analysis according to the Enrichment score.

2.4. Cell culture

The BEAS-2B normal human bronchial epithelial cell line, along with the A549 and H1299 lung cancer cell lines, were sourced from the American Type Culture Collection (ATCC, Manassas, VA, USA) and grown in RPMI-1640 medium (Gibco, #11875093) containing 10 % fetal bovine serum (FBS; Gibco, #10099141), 100 IU/mL penicillin, and streptomycin (60162ES76, Yeasen). They were cultured in a 37 °C, 5 % CO_2 incubator (Thermo Scientific, USA), and logarithmic phase cells were collected for experiments.

2.5. Cell transfection

Cells were transfected with small hairpin RNA (shRNA) targeting PLCD3 (shPLCD3) or a non-targeting control shRNA (shCtrl) using Lipofectamine 2000 (Invitrogen, #11668019) according to the manufacturer's instructions. When the cell fusion reached 70 %–80 %, 10 μmol/L pcDNA-vector and pcDNA-PLCD3 (forward: 5′-GCTTGGTACCGAGCTCGGATCCGCCACCATGCTGTGCGGCC-3′, reverse: 5′-TGCTGGATATCTGCAGAATTCTCAGGAGCGCTGGATGCGGATTTGGATGA-3′) were mixed with 10 μL Lipofectamine 2000 according to the instructions, and then added to the EP tube containing 50 μL Opti-MEM medium. After standing for 20 min, it was added to the cells. After 6 h, the medium was replaced with RPMI-1640 medium containing 10 % fetal bovine serum and antibiotics, and the cells were cultured for another 48 h. The cells were collected to check the transfection efficiency.

2.6. qRT-PCR

Total RNA was extracted using TRIzol (Invitrogen, #15596026), and all RNA samples were dissolved in DEPC water. The purity and concentration of total RNA were detected using a NanoDrop ND-1000. Prime Script RT reagent kit (Takara, #RR037A) was used to reverse transcribe cDNA using total RNA as a template. 1.0 μl of cDNA was mixed with 5.0 μl of SYBR Green qPCR Master Mix (#A25742), 0.4 μl of upstream and downstream primers each, and 3.2 μl of DEPC water to a total volume of 10 μl. The mixed system was added to a 96-well plate and qPCR was performed using the LightCycler 480 real-time PCR system. Each reaction was tested at

least three times. The primer sequences were shown in Table 1. The PCR reaction conditions were as follows: pre-denaturation at 94 °C for 3 min; denaturation at 94 °C for 15 s, extension at 62 °C for 40 s, for a total of 40 cycles. Non-specific amplification was detected by melting curve analysis, and the relative expression level was calculated using the $2^{-\Delta\Delta Ct}$ method.

2.7. Western blot

Proteins were extracted using RIPA lysis buffer (Thermo Fisher Scientific, #89900), and the lysate was added to SDS-PAGE sample loading buffer. Protein levels were measured with the BCA Protein Assay Kit from Thermo Fisher Scientific (catalog number 23225). Following a 5-min boil, SDS-PAGE electrophoresis was conducted and the sample was transferred onto a polyvinylidene fluoride membrane (Millipore, #IPVH00010). The membrane was blocked in a blocking buffer containing skim milk and TBST at room temperature for 2 h. The primary antibody was incubated overnight at 4 °C. The dilution of the primary antibody included PLCD3 (ab151594, Abcam, 1:1000), Rap1 (ab187659, 1:1000), b-Raf (ab308176 1:1000), GLUT1 (ab115730, Abcam, 1:1000), HK1 (ab154839, Abcam, 1:1000), HK2 (ab209847, Abcam, 1:1000), PKM2 (ab85555, Abcam, 1:1000) were added. The β-actin primary antibody (ab8226) was set as loading control (Use a concentration of 1 μg/ml, 1:1000). Following three washes of the membrane with TBST, it was left to incubate with the appropriate secondary antibody. Protein bands were visualized using an ECL detection system (Thermo Fisher Scientific, #32106).

2.8. Cell proliferation assay

Lung cancer cells were uniformly distributed at 2000 cells per well in a 96-well plate. Following a 48-h incubation period, each well received 20 μL of MTT (C0009S, Beyotime Biotechnology, China) at a concentration of 5 g/L. After incubation for 4 h, the supernatant was discarded. 150 μL of dimethyl sulfoxide (DMSO; Sigma-Aldrich, #D2650) was added to each well, and the absorbance value at 570 nm was measured using an ELISA reader. The experiment was set up with six parallel samples.

2.9. EdU (5-Ethynyl-2′-deoxyuridine) integration test

1×10^4 A549 cells/mL were seeded in a 96-well culture plate. Following the kit's guidelines, a 10 μmol/L EdU solution was introduced into each well. The cells were treated with 4 % paraformaldehyde following a 2-h incubation at 37 °C. The cells underwent permeabilization using 0.3 % Triton X-100 for a duration of 3 min. Following the removal of the permeabilization solution, 50 μL of the prepared Click reaction mixture was introduced to each well and left to incubate in the dark at room temperature for 30 min. The Click reaction mixture (C0078S, BeyoClick™ EdU, Beyotime Biotechnology, China) was removed, followed by three PBS washes of the cells. Each well received DAPI (Invitrogen, #D1306). The cells were observed and counted under a Nikon Eclipse Ti-E fluorescence microscope. To determine the percentage of EdU-positive cells. A minimum of five randomly selected fields per well.

2.10. Transwell chamber assay for cell invasion capability

A549 and NCI-H1299 cells were cultured overnight in serum-free DMEM medium. Allow the Matrigel to hydrate at room temperature for 15–30 min, then remove the remaining culture medium. After 24 h of starvation treatment, add 100 μl of serum-free culture medium to the upper chamber of the Transwell (Corning, #3422) coated with Matrigel (BD Biosciences, #356234). Add 600 μl of DMEM containing 10 % fetal bovine serum to the lower chamber. Incubate at 37 °C with 5 % CO2 for 1 h. Seed cells at a concentration of 5×10^5 cells/ml in the upper chamber. After 24 h of incubation, gently wipe the Matrigel and cells inside the chamber with a cotton swab. Fix with 90 % ethanol and stain with 1 % crystal violet (Sigma-Aldrich, #C0775). Using a light microscope, capture images of five randomly chosen high-magnification areas, and count the cells that have traversed the membrane.

2.11. Cell clonogenic ability

Cells were treated with trypsin to create single-cell suspensions and then plated in 6-well dishes at a concentration of 500 cells per well. For 14 days, cells were grown in RPMI-1640 medium with 10 % FBS, and the medium was refreshed every three days. The colonies were treated with 4 % paraformaldehyde for a quarter of an hour and then stained with 0.1 % crystal violet for the same duration. Microscopic examination was used to count colonies that had over 50 cells. The test was conducted three times, and the colony formation percentage was determined.

Table 1
The primer sequences used in this study.

	Forward	Reverse
HK1	TGGAGGAGGAGGAGGAGGAG	GGTGGTGGTGGTGGTGGTGA
GLUT1	GGAGTGTGGAGGAGGAGGAG	GGTGGTGGTGGTGGTGGTGA
PKM2	ATGGCTGACACATTCCTGGAGC	CCTTCAACGTCTCCACTGATCG
HK2	GAGTTTGACCTGGATGTGGTTGC	CCTCCATGTAGCAGGCATTGCT
β-actin	TGGCACCCAGCACAATGAA	CTAAGTCATAGTCCGCCTAGAAGCA

2.12. Glucose uptake and consumption detection

Logarithmic phase cells were seeded in a 96-well culture plate. The supernatant from each cell group was collected, and the glucose levels in the medium were measured with a glucose assay kit. The glucose consumption of each group of cells was calculated based on the blank group. The glucose consumption of the treated group was compared with that of the control group to observe the effect of different treatments on glucose uptake by lung cancer cells.

2.13. Lactate content detection

Prepare a standard solution according to the instructions of the lactate content detection kit to draw a standard curve. After collecting the cell supernatant, add lactate buffer, lactate dehydrogenase mixture, and lactate substrate mixture in order. After mixing well, incubate in the dark for 30 min. The absorbance value at 450 nm of each well was detected using an ELISA reader. Draw a standard curve with the standard solution concentration on the X-axis and the corresponding D value on the Y-axis, and obtain the standard curve equation. Substitute the D value of each group of cells to calculate the lactate content (μmol/ml). Draw a standard curve with the standard solution concentration on the X-axis and the corresponding D value on the Y-axis, and obtain the standard curve equation. Substitute the D value of each group of cells to calculate the lactate content (μmol/ml). Use the Blank group as the standard, and express the relative lactate content in the cell supernatant as the ratio of the experimental group to the Blank group.

2.14. Seahorse assay for measuring glycolytic metabolic flux

Cells were seeded in Seahorse XF96 cell culture microplates (Agilent Technologies, Santa Clara, CA, USA) at a density of 10,000 cells per well and allowed to adhere overnight. Cells were transfected with shPLCD3, OE-PLCD3, or control plasmids using Lipofectamine 2000 (Life Technologies, Rockville, MD, USA) according to the manufacturer's instructions. After 6 h, the medium was replaced with fresh RPMI-1640 medium containing 10 % FBS and antibiotics, and cells were cultured for an additional 48 h. The Seahorse XF Glycolysis Stress Test was performed using the Seahorse XF96 Analyzer (Agilent Technologies). The culture medium was replaced with Seahorse XF Base Medium supplemented with 2 mM L-glutamine (pH 7.4), and cells were incubated at 37 °C in a non-CO_2 incubator for 1 h to allow temperature and pH equilibration. ECAR was measured to establish the baseline glycolytic activity. 10 mM glucose was injected to stimulate glycolysis, and the ECAR was measured to determine the glycolytic rate. 1 μM oligomycin was injected to inhibit ATP synthase, thereby shifting the energy production to glycolysis, and the ECAR was measured to determine the glycolytic capacity. 50 mM 2-DG, a glycolysis inhibitor, was injected to confirm the specificity of the glycolytic response, and the ECAR was measured to determine the non-glycolytic acidification.

2.15. MitoSOX red assay for measuring mitochondrial oxidation

Cells were placed in 6-well plates (200,000 cells per well) and left to attach overnight. A 5 mM stock solution of MitoSOX Red mitochondrial superoxide indicator (Thermo Fisher Scientific, M36008) was made in DMSO. The effective mixture was created by diluting the original solution to achieve 5 μM in HBSS (Hank's Balanced Salt Solution) lacking calcium and magnesium. The cells were subsequently exposed to 1 mL of MitoSOX Red solution per well at 37 °C for 10 min, ensuring they were shielded from light. The cells were visualized with a Olympus fluorescence microscope (IX73, Tokyo, Japan) that included a Texas Red filter set (excitation at 510 nm, emission at 580 nm). Photos were taken with a digital camera (Olympus DP80) and examined using ImageJ software (NIH, Bethesda, MD, USA).

2.16. Nude mouse subcutaneous transplantation tumor model

Eighteen healthy nude mice (BALA/c, Beijing Laboratory Animal Research Center, Beijing, China) were randomly divided into three groups: shCtrl, sh-PLCD3, and sh-PLCD3+PKC, with six nude mice in each group. The cells were cultured in RPMI1640 medium containing 10 % fetal bovine serum. They were cultured at 37 °C, 5 % CO_2, and saturated humidity. Logarithmic phase A549 cells were taken and digested with trypsin. After centrifugation to remove the supernatant, the cells were resuspended in 0.9 % sodium chloride solution. A cell suspension of 1×10^6 cells/mL was prepared. 0.1 mL (2×10^5) was taken and inoculated subcutaneously in nude mice. Observe the growth of the tumor in nude mice. The maximum and minimum diameters of the tumor were measured every 5 days, and the tumor volume was calculated. The formula for calculating tumor volume is: VT = 1/2ab2, where a and b are the maximum and minimum diameters, respectively. After a month, the nude mice were put down, and the tumor samples were collected, weighed, and the rate of tumor suppression was determined. The hairless mice received an intraperitoneal injection of pentobarbital sodium at a dosage of 150 mg/kg body weight. The animal studies adhered to ethical standards and received approval from the Animal Care Ethics Committee of Tianjin First Central Hospital (2022-05-A5), fulfilling the ethical welfare criteria for animal research.

2.17. Statistical analysis

All in vitro experiments were repeated three times independently. For the in vivo mouse experiment, a single trial was conducted with 6 mice per group. GraphPad Prism 8.0 was utilized to conduct the statistical evaluations. Quantitative data with a normal distribution were represented as the average ± standard deviation. An unpaired two-tailed Student's t-test was employed for comparing
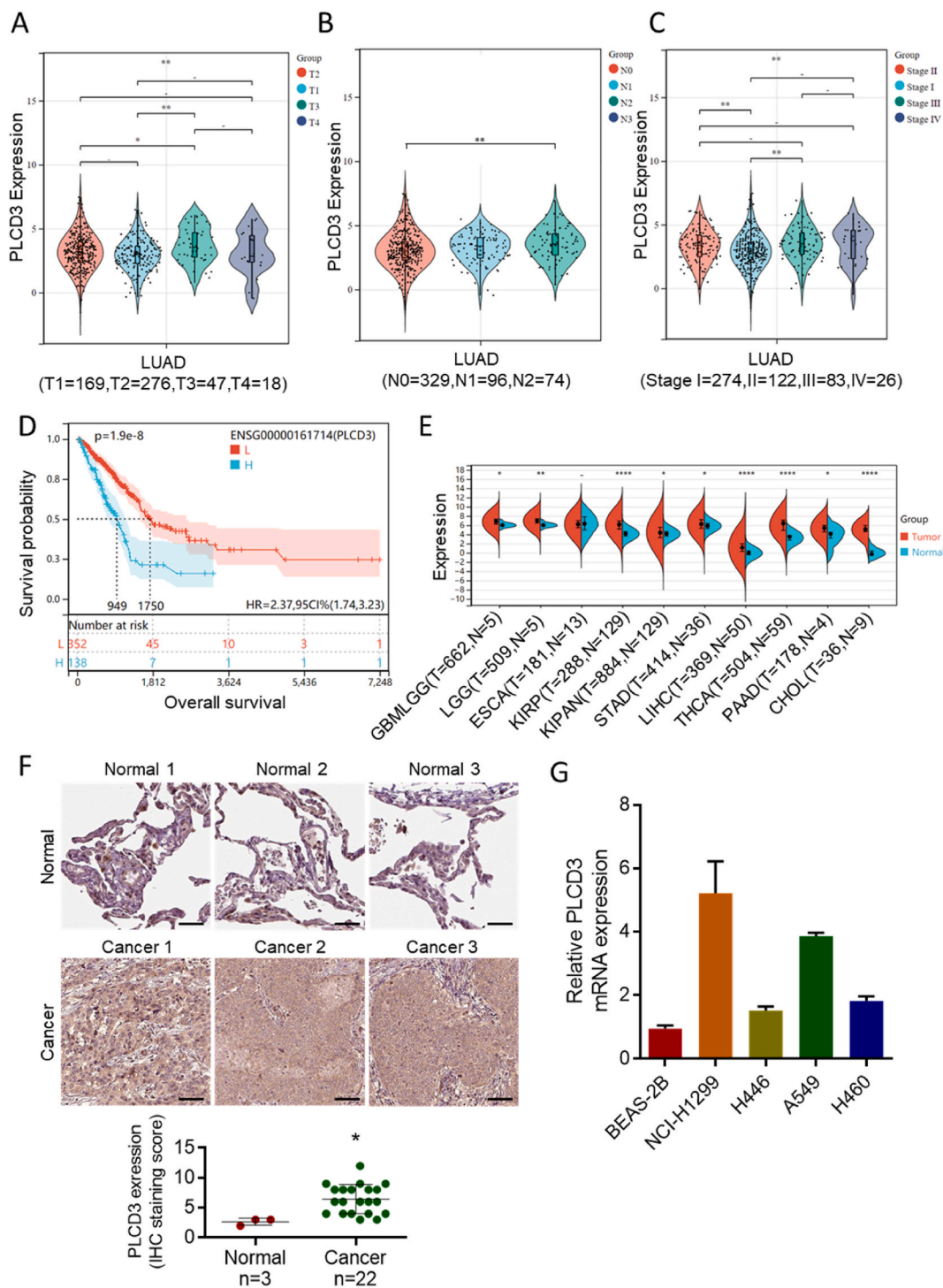
Fig. 1. PLCD3 is upregulated and associated with poor prognosis in lung cancer. A-C. Bioinformatics analysis of PLCD3 in LUAD (A) Relationship between PLCD3 expression and T stage; (B) PLCD3 expression and N stage relationship; (C) PLCD3 expression and stage relationship D. Kaplan-Meier analysis was performed on the overall survival rate related to PLCD3 expression, and the P value was tested by log rank. E. TCGA data analysis of PLCD3 in other tumors and normal peritumoral tissues. F. Immunohistochemical staining analysis of PLCD3 in normal lung tissue and lung cancer tissue samples. G. Quantitative RT-PCR analysis of PLCD3 expression in normal lung epithelial cells (BEAS-2B) and lung cancer cell lines. All data were shown as the mean ± SD, n = 3, *p < 0.05, **p < 0.01.
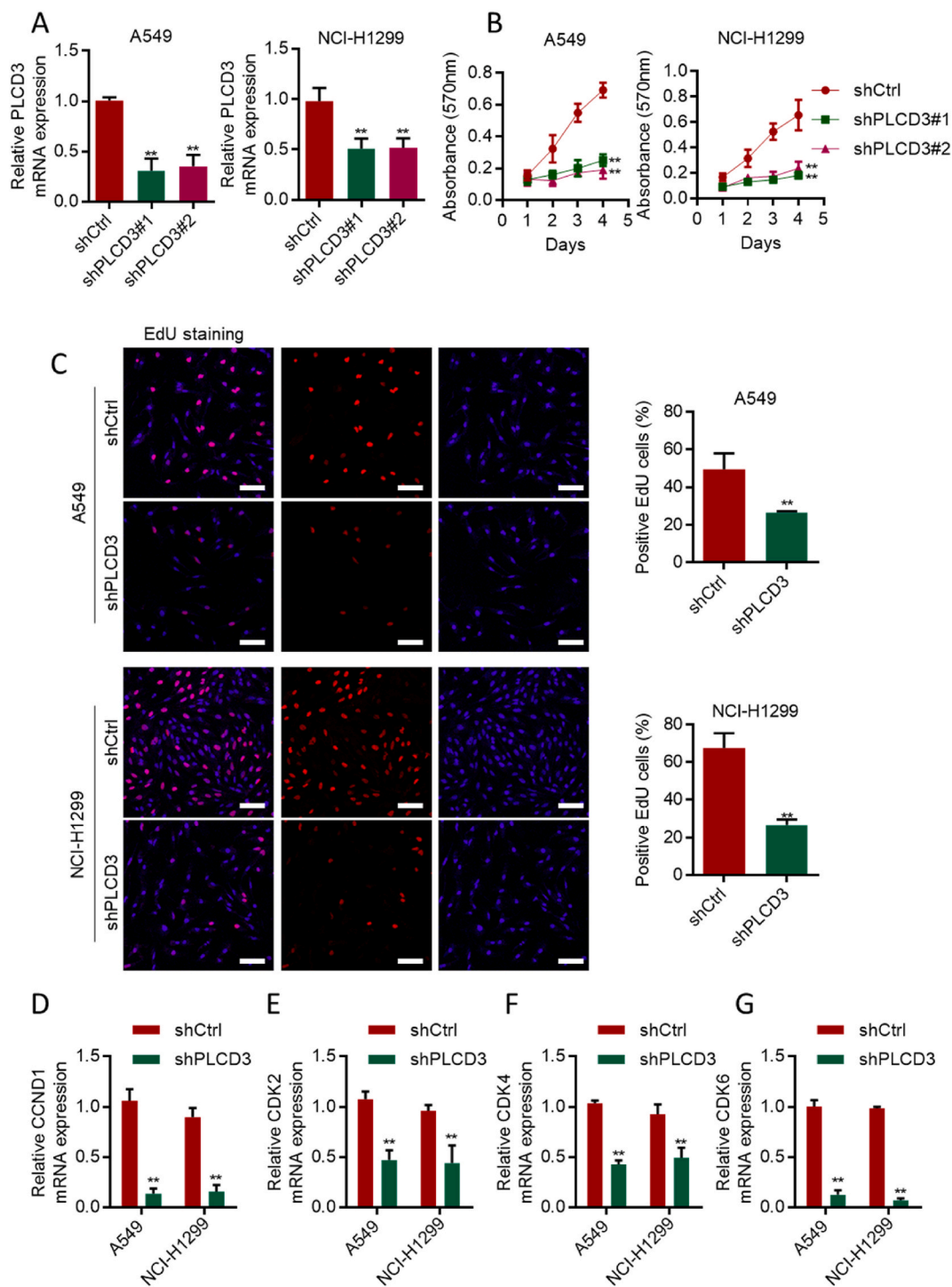
Fig. 2. PLCD3 promotes cell proliferation by regulating cell cycle processes. A. Analysis of PLCD3 expression in A549 and NCI-H1299 cells transfected with PLCD3 shRNA clones or shRNA scrambled. B. The effect of PLCD3 on the proliferation of lung cancer cells was detected by MTT assay. C. Image and quantitative analysis of EdU-stained positive lung cancer cells. D-G. Analysis of mRNA expression levels of cell cycle-related proteins in lung cancer cells with or without PLCD3 silencing. (D) *CCND1*; (E) *CDK2*; (F) *CDK4*; (G) *CDK6*. All data were shown as the mean ± SD, n = 3, *p < 0.05, **p < 0.01.

the two groups. To compare several groups, a one-way ANOVA was conducted, followed by Tukey's post hoc analysis. A p-value less than 0.05 was deemed to indicate statistical significance. All graphs were generated using GraphPad Prism 8.0.

3. Results

1 The PLCD3 gene is highly expressed in lung cancer tissues and cells.

Firstly, the difference in *PLCD3* mRNA expression levels between lung cancer tissues and normal lung tissues was analyzed using the TCGA public database. The results in Fig. 1A–C showed that high expression of PLCD3 is associated with lung cancer T, N, and Stage. PLCD3 expression levels are also associated with the prognosis of lung cancer patients. Compared with the low expression group, the overall survival time of lung cancer patients in the high expression PLCD3 group is longer (P < 0.01, Fig. 1D). TCGA database analysis also showed that the PLCD3 gene is highly expressed in various tumors such as GBM, KIRP, STAD, and LIHC (Fig. 1E). Further immunohistochemical analysis showed that PLCD3 expression is elevated in lung cancer tumor tissues (Fig. 1F). Statistical analysis showed that PLCD3 protein expression is upregulated in lung cancer tissues compared to adjacent tissues. PLCD3 in lung cancer cell lines is also increased to varying degrees compared to normal lung epithelial cells (BEAS-2B) (Fig. 1G). A549 and NCI-H1299 cells, which have relatively high expression of PLCD3, were selected for further study.

2 Silencing PLCD3 expression can inhibit the proliferation of lung cancer cells.

After transfection with sh-PLCD3, PLCD3 in LC cells were decreased compared to the sh-Ctrl group (P < 0.01, Fig. 2A). LC cells were treated with PLCD3, and the effects on cell proliferation and activity were observed through MTT and EdU experiments. Sh-PLCD3 treatment can inhibit the proliferation ability of lung cancer cells (Fig. 2B–C). These results have demonstrated that silencing PLCD3 expression can inhibit the proliferation of lung cancer cells. It is speculated that the mechanism by which PLCD3 regulates cell activity may be related to its regulation of cell cycle-related genes. qRT-PCR experiments showed that silencing PLCD3 can inhibit the expression of CCND1, CDK2, CDK4, and CDK6 in LC cells (Fig. 2D–G). To investigate the role of PLCD3 in the progression of lung cancer, we first overexpressed PLCD3 in lung cancer cell lines. Western blot analysis showed that PLCD3 protein in cells transfected with the PLCD3 overexpression plasmid was upregulated (Fig. S1A). This provides a reliable experimental basis for subsequent experiments. We then assessed the impact of PLCD3 overexpression on the proliferation, migration, and invasion abilities of lung cancer cells. EdU staining results indicated that PLCD3 overexpression promoted the proliferation of LC cells (Fig. S1B). Furthermore, Transwell assay results demonstrated that PLCD3 overexpression markedly enhanced the migration and invasion capabilities of these two lung cancer cell lines (Fig. S1C). These findings suggest that PLCD3 plays an important role in promoting the malignant phenotype of lung cancer cells. Considering the critical role of metabolic reprogramming in cancer progression, we further studied the effect of PLCD3 on glucose metabolism in lung cancer cells. The experimental results showed that PLCD3 overexpression increased glucose uptake (Fig. S1D) and consumption (Fig. S1E) in LC cells. Simultaneously, PLCD3 overexpression also led to a significant increase in lactate production (Fig. S1F) and lactate dehydrogenase activity (Fig. S1G). These results collectively indicate that PLCD3 promotes aerobic glycolysis, also known as the Warburg effect, in lung cancer cells.

3 PLCD3 regulates the metabolic reprogramming of lung cancer cells through the activation of the Rap1 pathway.

GO analysis showed that PLCD3 and its co-expressed genes are mainly involved in glucose transport and energy metabolism processes in lung cancer (Fig. 3A). Result of Fig. 3B demonstrate that shPLCD3 treatment reduced PLCD3 expression, while shPLCD3 + OE-PLCD3 treatment was able to upregulate PLCD3 expression (Fig. S2). Further experiments showed that silencing PLCD3 in LC cells can reduce glucose uptake and consumption, as well as lactate accumulation and LDH activity (Fig. 3C–F). Additionally, we supplemented mitochondrial oxidation experiments (Fig. 3G) using the MitoSOX Red mitochondrial superoxide probe to detect the degree of mitochondrial oxidation. The results showed that silencing PLCD3 reduced mitochondrial function in LC cells, while co-transfection with shPLCD3+OE-PLCD3 upregulated mitochondrial function in LC cells. The mRNA expression of glucose transport protein 1 (*GLUT1*), *HK1*, *HK2*, and *PKM2* in LC cells was also decreased after transfection with sh-PLCD3 plasmids (Fig. 3H–K). Furthermore, we measured the glycolytic metabolic flux using the Seahorse assay. The experimental results showed that silencing PLCD3 reduced the energy metabolism capacity of LC cells, while co-transfection with shPLCD3+OE-PLCD3 upregulated the energy metabolism capacity of LC cells. These results further support the role of PLCD3 in regulating glycolytic reprogramming (Fig. 3L). The impact of PLCD3 on glycolysis in PC cells was investigated using the Seahorse XF extracellular flux analyzer. We found that PLCD3 knockdown reduced glycolysis and glycolytic capacity in PC cells, while enhancing ATP production and maximal respiration (Fig. S3). The results shown in Fig. 3M indicate that, compared to the shCtrl + OE-Ctrl group, the invasion ability of A549 and H1299 cells is reduced after the sh-PLCD3. However, with the re-overexpression of PLCD3, the invasion capability of the cells is enhanced, approaching that of the control group.

4 PLCD3 can promote aerobic glycolysis and cell growth by activating the Rap1 pathway

KEGG enrichment analysis showed that PLCD3 may regulate the Rap1 signaling pathway (Fig. 4A). Western blot experiments confirmed that PLCD3 can regulate the protein expression levels of Rap1, b-Raf, GLUT1, HK1, HK2, and PKM2 protein in LC cells (Fig. 4B & Fig. S4). To investigate whether PLCD3 exerts its effects through the Rap1 signaling pathway in lung cancer cells, LC cells
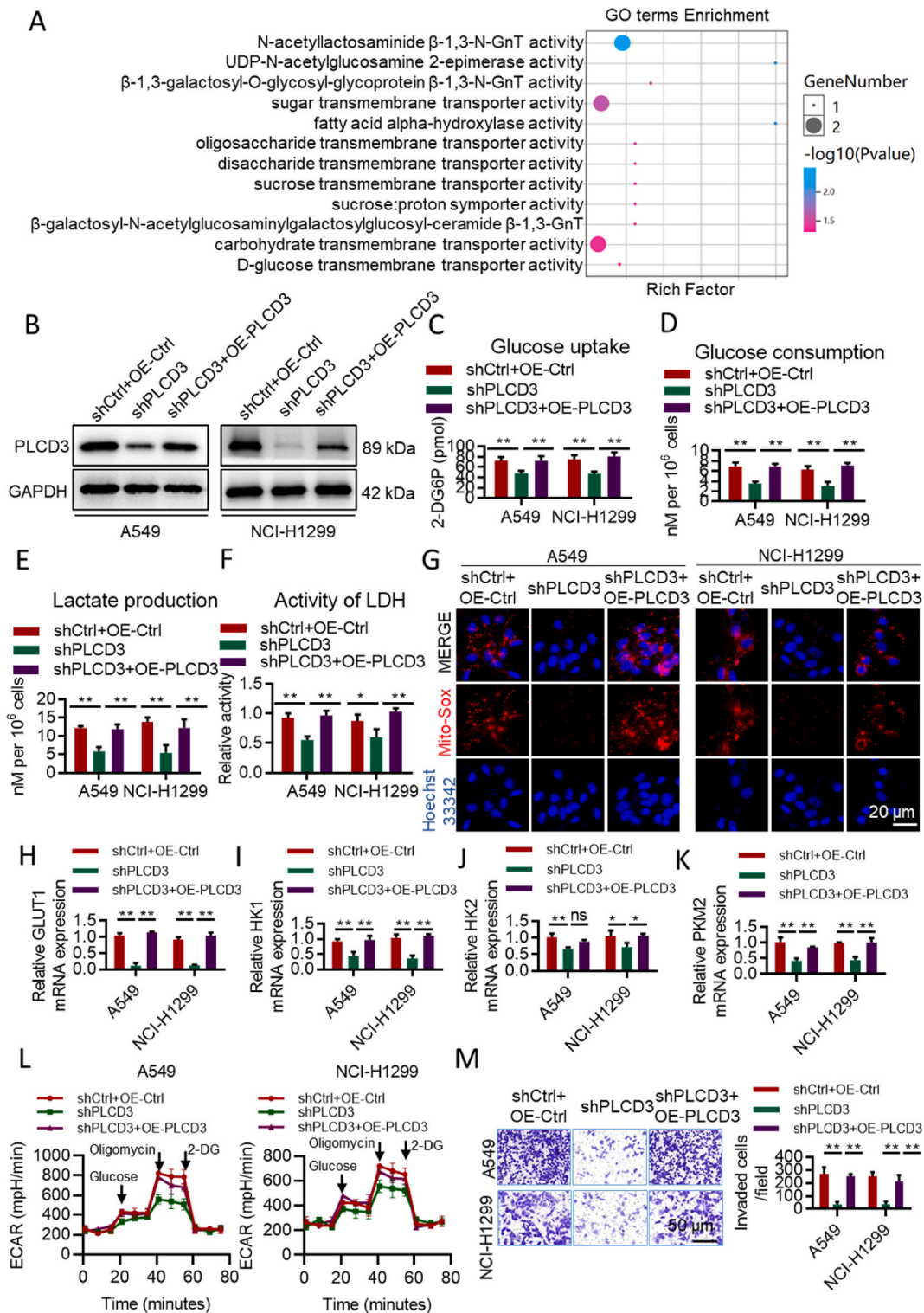
Fig. 3. PLCD3 regulates glycolytic reprogramming in lung cancer cells. A. GO enrichment analysis shows significant enrichment of gene sets involved in glucose metabolism-related functions in cells. B. Western blot data of PLCD3 with or without PLCD3 silencing and PLCD3 restoration. C. Glucose uptake by lung cancer cells with or without PLCD3 silencing and PLCD3 restoration. D. Glucose consumption in lung cancer cells with or without PLCD3 silencing and restoration of PLCD3. E. Lactate production in lung cancer cells with or without PLCD3 silencing and PLCD3 restoration. F. Lung cancer cell lactate dehydrogenase activity with or without PLCD3 silencing and restoration of PLCD3. G. Mitochondrial oxidation experiments using the MitoSOX Red mitochondrial superoxide probe to detect the degree of mitochondrial oxidation. H-K. Quantitative RT-PCR

analysis of the levels of key glycolysis-related enzymes in A549 cells after PLCD3 silencing and restoration. (H) GLUT1; (I) HK1; (J) HK2; (K) PKM2 L. Glycolytic metabolic flux using the Seahorse assay. M. The effect of PLCD3 on the invasion of lung cancer cells was detected by transwell assay. All data were shown as the mean ± SD, n = 3, *p < 0.05, **p < 0.01. (For interpretation of the references to colour in this figure legend, the reader is referred to the Web version of this article.)

were treated with OE-PLCD3 for 48 h, followed by treatment with 1 μmol/L GGTI298 (a Rap1 inhibitor) for 6 h. Further experiments showed that overexpression of PLCD3 can activate the Rap1 pathway and promote cell activity, while the addition of a Rap1 inhibitor can reduce cell activity and glucose uptake and consumption (Fig. 4C–E). qRT-PCR experiments also showed that the expression of GLUT1, HK1, HK2, and PKM2 in LC cells was upregulated after overexpression of PLCD3 and downregulated after the addition of a Rap1 inhibitor (Fig. 4F–I). The results in Fig. 4J indicate that, compared to the Ctrl + DMSO group, overexpression of PLCD3 increased the invasive abilities of A549 and H1299 cells. However, this invasive ability was reduced upon administration of GGTI298.

5 PLCD3 can activate the Rap1 pathway by directly promoting PKC expression

The results described above have demonstrated that increasing PLCD3 expression can promote the progression of lung cancer cells and regulate their energy metabolism. It is speculated that the mechanism by which PLCD3 regulates cell malignant progression may be related to its regulation of energy metabolism. It is known that PKC is an important molecule involved in regulating mitochondrial energy metabolism, and TCGA lung cancer data shows a positive correlation between PLCD3 and PKC expression (Fig. 5A). Immunoblotting experiments showed that silencing PLCD3 can reduce the expression of PKC in lung cancer cells, and changing the expression of PLCD3 can also affect Rap1 and b-Raf. Overexpression of PKC can reverse the inhibitory effect of silencing PLCD3 on the Rap1 pathway (Fig. 5B & Fig. S5). The protein expression levels of GLUT1, HK1, HK2, and PKM2 protein were also upregulated after overexpression of PKC in LC cells transfected with sh-PLCD3 plasmids (Fig. 5C–F). These results suggest that PLCD3 may regulate the energy metabolism of lung cancer cells by directly promoting PKC and activating the Rap1 pathway.

6 PLCD3 promotes aerobic glycolysis in a PKC-dependent manner

GF109203X is a selective PKC inhibitor that can inhibit the activity of multiple PKC subtypes. The results showed that, the glucose uptake and consumption in the sh-PLCD3 group and sh-PLCD3+PKC + GF109203X group were reduced, while the glucose uptake and consumption in the sh-PLCD3+PKC group were increased (Fig. 6A–B). Lactate accumulation and LDH activity were also reduced in the sh-PLCD3 group and sh-PLCD3+PKC + GF109203X group, while they were increased in the sh-PLCD3+PKC group (Fig. 6C–D). glucose transporters and glycolytic enzymes such as GLUT1, HK1, HK2, and PKM2 were decreased after silencing PLCD3, and were upregulated in the sh-PLCD3+PKC group. The addition of the PKC inhibitor GF109203X further reduced these enzymes (Fig. 6E–H). These results suggest that overexpression of PKC can reverse the inhibitory effect of sh-PLCD3 on glucose metabolism in LC cells. The results of Fig. 6I show that compared to the shCtrl group, the clonogenic ability of A549 and H1299 cells was reduced after silencing PLCD3. However, the clonogenic ability was enhanced and approached that of the control group after re-expressing PKC. Nevertheless, the addition of GF109203X further reduced the clonogenic ability compared to the sh-PLCD3+PKC group.

7 PLCD3-PKC axis promotes lung tumor development by regulating glycolysis

Subcutaneous tumor experiments were performed using A549 cells with PLCD3 deficiency and PKC restoration to investigate the effect of the PLCD3-PKC axis on lung cancer development. In the experiment, nude mice were injected with A549 single-cell suspensions, and a slight protrusion was observed on the 4th day. There were no significant differences in diet and water intake among the groups, and no deaths occurred. The tumor long and short diameters of the nude mice were measured starting from the 10th day. The control group had the fastest increase in tumor volume, while the other groups showed varying degrees of increase. The nude mice were euthanized on the 30th day. The results showed that the growth of lung cancer tumors was inhibited after knocking out PLCD3, while it was enhanced after overexpressing PKC (Fig. 7A). Further analysis of glycolytic enzymes in tumor tissues showed that compared to the shCtrl group, PLCD3 and PKC were decreased after transfection with sh-PLCD3. However, PLCD3 did not change after overexpression of PKC (Fig. 7B–C). glycolytic enzymes in tumor tissues showed that silencing PLCD3 inhibited the expression of GLUT1, HK1, HK2, and PKM2, while overexpression of PKC restored their expression (Fig. 7D–G). TCGA lung cancer patient data showed a positive correlation between PLCD3 expression and the expression of PKC, HK1, HK2, and PKM2 (Fig. 7H). These findings suggest that the PLCD3-PKC axis plays a critical role in regulating energy metabolism and promoting lung tumor development.

4. Discussion

Glycolysis reprogramming is the most representative metabolic characteristic in tumors [15]. Tumor cells have a unique energy metabolism pathway. Even under aerobic conditions, they do not use mitochondrial oxidative phosphorylation to produce energy, but exhibit active aerobic glycolysis, known as the Warburg effect (aerobic glycolysis) [16,17]. Increasing evidence has shown that the aerobic glycolysis pathway of tumor glucose is a potential target for tumor treatment [18,19].

Due to the cross-redundancy of signaling pathways regulating tumor growth and normal cell proliferation, it is generally believed that cancer driver genes cannot be targeted to regulate tumors. Instead, abnormal metabolism in cancer cells can be targeted to control
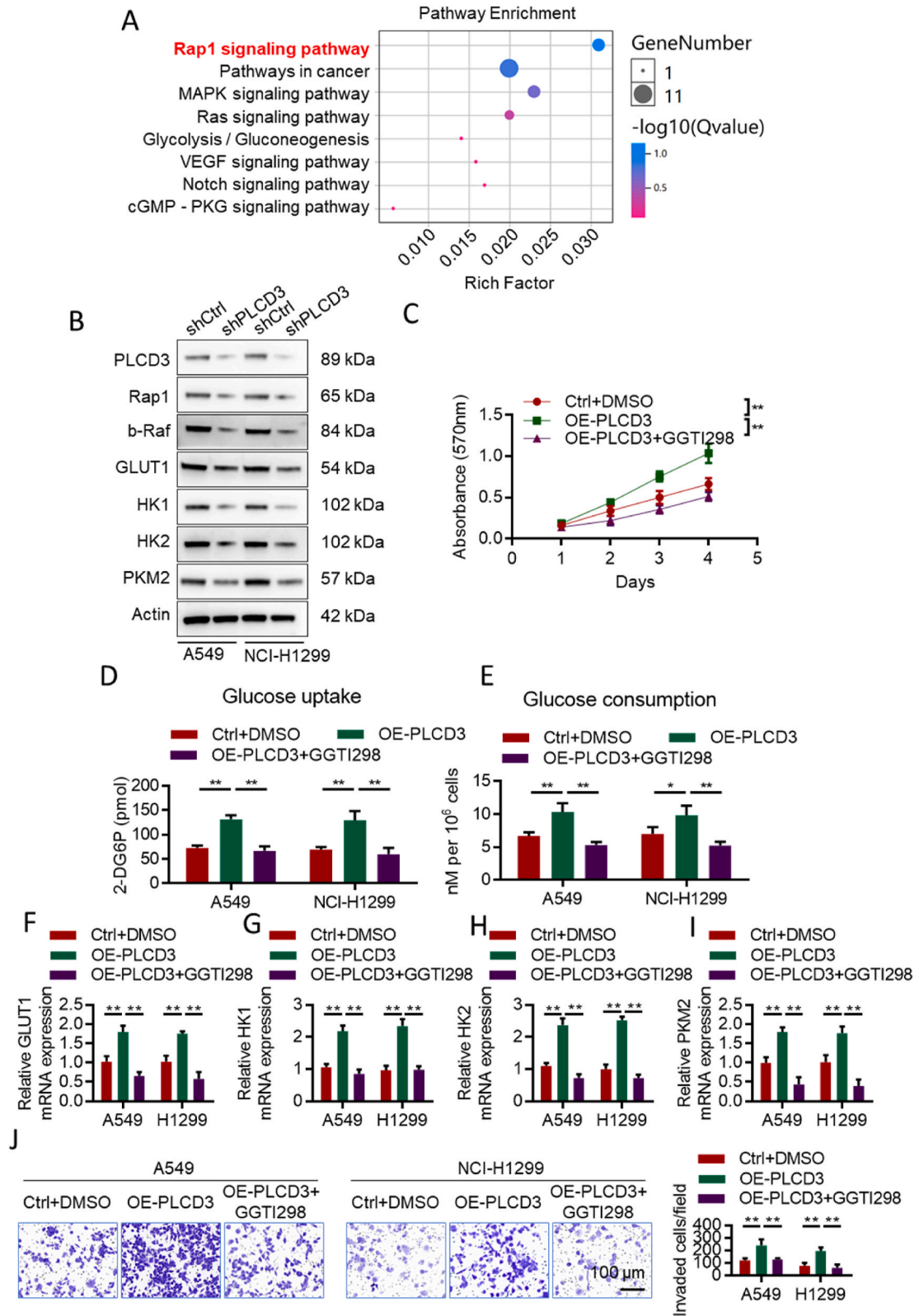
(caption on next page)

Fig. 4. PLCD3 promotes aerobic glycolysis and cell growth through activation of the RAP1 pathway. A. KEGG shows significant enrichment of RAR1 pathway-related genes. B. Western blot analysis of Rap1, b-Raf, GLUT1, HK1, HK2, and PKM2 in lung cancer cells with or without PLCD3 silencing. C. Growth assay of A549 cells with and without PLCD3 induction and XIV induction. D–E. Glucose uptake and consumption assays in A549 and NCI-H1299 cells with or without PLCD3 induction and 1 μmol/L GGTI298 (Rap1 inhibitor) treatment. F-I. Detection of the mRNA expression levels of *GLUT1*, *HK1*, *HK2* and *PKM2* in A549 and NCI-H1299 cells transfected or not transfected with PLCD3 and GGTI298. (F) *GLUT1*; (G) *HK1*; (H) *HK2*; (I) *PKM2*. J. The effect of PLCD3 and GGTI298 on the invasion of lung cancer cells was detected by transwell assay. All data were shown as the mean ± SD, n = 3, *p < 0.05, **p < 0.01.
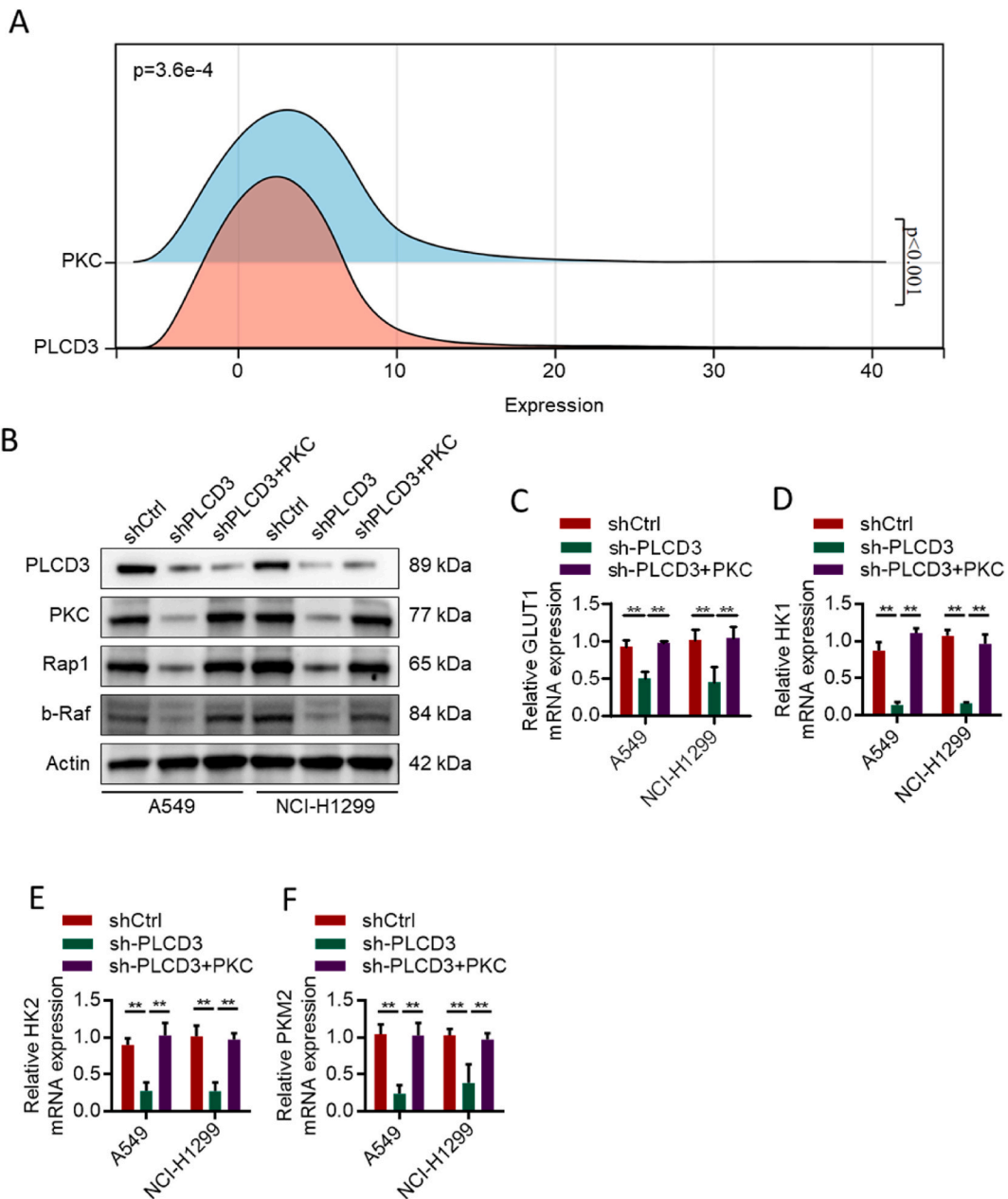

Fig. 5. PLCD3 regulates the RAP1 pathway through PKC. A. Mountain plot analysis of co-expression correlation of PLCD3 and PKC in lung cancer tumor tissues. B. Immunoblot detection of PLCD3, PKC, Rapl, b-Raf in lung cancer cells with or without PLCD3 silencing and PKC restoration. C-F. Analysis of GLUT1, HK1, HK2 and PKM2 in PLCD3-silenced and PLCD3-restored lung cancer cells. All data were shown as the mean ± SD, n = 3, *p < 0.05, **p < 0.01.
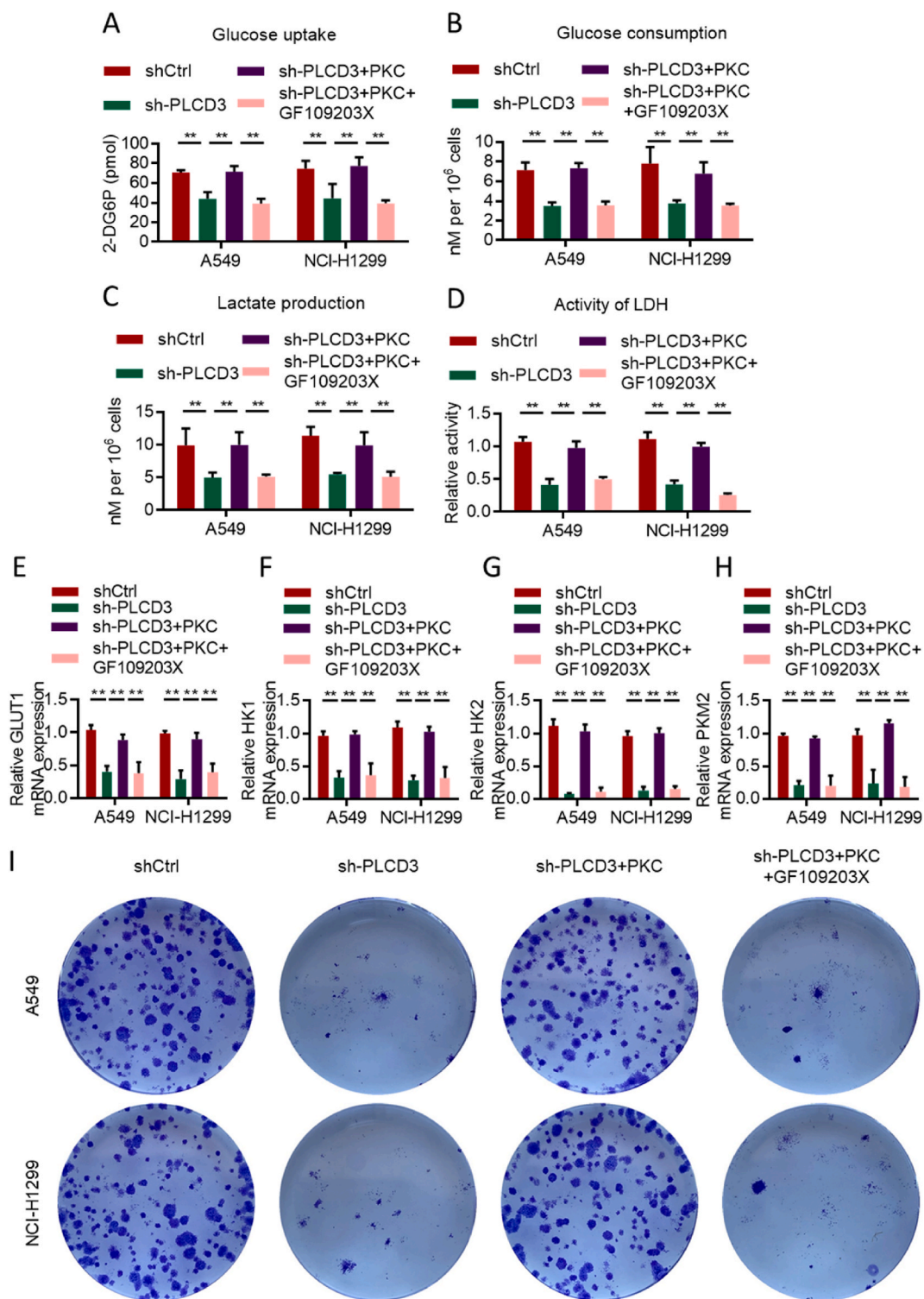
Fig. 6. PLCD3 promotes aerobic glycolysis in a PKC-dependent manner. A. Effects of different treatments on glucose uptake in lung cancer cells. B. Glucose consumption of lung cancer cells under different treatments. C. Lactate production in differently treated lung cancer cells. D. Effects of different treatments on the activity of lactate dehydrogenase in lung cancer cells. E-H. Detection of GLUT1, HK1, HK2 and PKM2 in shCtrl, shPLCD3 and shPLCD3/PKC cells treated with or without GF109203X. I. Plate Colony Formation Assay to Test Cell Clonogenic Ability. All data were shown as the mean $\pm$ SD, n = 3, *p < 0.05, **p < 0.01.
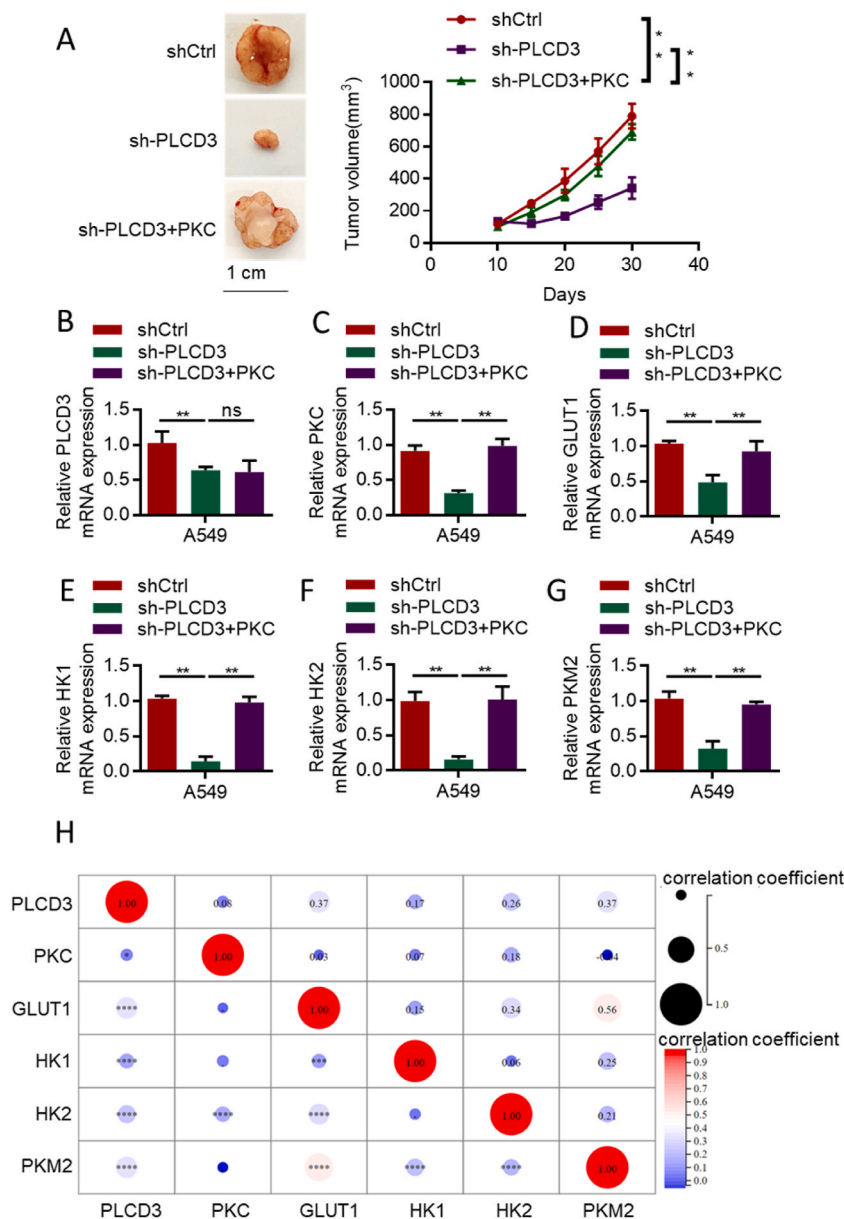
Fig. 7. The PLCD3-PKC axis promotes lung tumorigenesis by regulating glycolysis. A. Restoration of subcutaneous tumorigenicity of A549 cells by deletion of PLCD3 and PKC. B. Analysis of PLCD3 expression in tumor tissues formed by PLCD3-deficient and PKC-recovered lung cancer cells C. Analysis of PKC expression in tumor tissues formed by PLCD3-deficient and PKC-recovered lung cancer cells D-G. Expression of GLUT1, HK1, HK2 and PKM2 in tumor tissues formed by PLCD3-deleted and PKC-recovered lung cancer cells H. Correlation of PLCD3 expression with PKC, HK1, HK2 and PKM2 in TCGA lung cancer patient data. All data were shown as the mean ± SD, n = 6, *p < 0.05, **p < 0.01.

cancer cell proliferation triggered by cancer signals [20]. Therefore, finding a way to cure cancer by regulating cancer metabolism may be a future research focus. The abnormal glucose metabolism in lung cancer cells is mainly manifested by the enhancement of the glycolysis pathway and the weakening of the mitochondrial oxidative pathway. The enhancement of the glycolysis pathway can provide sufficient ATP and metabolic substances to support the proliferation and invasion of lung cancer cells. In addition, the enhancement of the glycolysis pathway can also produce a large amount of lactate, leading to tumor acidification, thereby promoting tumor invasion and metastasis [21].

Protein kinase C (PKC) encompasses a broad group of serine/threonine kinases, each with unique structural and functional properties [22]. PKC is also a key link in a series of cell cascade signal transduction pathways. PKC plays an important regulatory role in some processes of tumor metastasis [23]. Downregulation of PKC activity can inhibit tumor metastasis [24]. However, there is no research on the relationship between PKC and the PLCD3 gene. This experiment explored the mechanism of action of PLCD3 and

whether there is a connection between it and the PKC signaling pathway. Earlier research indicates a connection between PKC expression and the growth and spread of tumors. The expression of PKC in high proliferation and metastasis cells is higher than that in low proliferation and metastasis cells. The findings of this study indicate that PKC is crucial in the mechanism by which PLCD3 enhances tumor growth. It further implies that the PLCD3 gene might control the Rap1 signaling route by influencing PKC expression. However, it is still worth further research to explore how the PLCD3 gene regulates the intracellular glucose metabolism process and in what way.

Oncogenes and tumor suppressor genes can affect tumor cell glucose metabolism through various mechanisms and are considered the primary factors leading to tumor occurrence and driving glucose metabolism reprogramming [25]. The oncogene KRAS can change the metabolic process of tumor cells in various ways, including enhancing the glucose uptake and glycolysis process of tumor cells, even if there is a large amount of oxygen in the tumor tissue (Warburg effect) [26]. As an important and unique member of the small G protein Ras family, Rap is not simply an inhibitory protein of Ras. In recent years, a large number of studies have shown that Rap not only promotes cell migration, polarization, proliferation, and differentiation, but also is related to the proliferation, invasion, and migration of malignant tumor cells in tumor cells. Mechanistic studies have shown that Ras can also regulate tumor cell glucose metabolism. Studies have shown that the effect of the KRAS gene on tumor metabolism can be achieved by transcriptionally regulating glucose transporters and glycolytic enzymes [27].

This study found that upregulating PLCD3 can promote the activity and protein expression levels of metabolic enzymes in the glycolysis pathway of tumor cells, including HK, PKM, and lactate dehydrogenase (LDH) [28,29]. HK is the first rate-limiting enzyme in glycolysis, which mainly includes five subtypes: HK1, HK2, HK3, HK4, and hexokinase domain-containing 1 (HKDC1). Among them, HK2 is abnormally highly expressed in various cancer cells, and high expression of HK2 is associated with poor prognosis in cancer patients. Related studies have shown that silencing HK2 expression can effectively reduce glycolysis activity [30]. PKM is a rate-limiting enzyme responsible for catalyzing the last step of glycolysis. PKM2 is highly expressed in tissues such as lung cancer, liver cancer, glioma, and renal cancer, and is closely related to tumor staging, clinical staging, prognosis, and other factors [31]. Recent studies have found that injecting the PKM2 inhibitor compound 3K into the tail vein of mice can inhibit the growth of transplanted tumors in mice, leading to cell death, thus confirming that reducing PKM2 expression can effectively inhibit tumor growth. Multiple studies have shown that reducing PKM2 expression can lead to cancer cell death, reduced metabolic activity, and reduced tumor occurrence. At the same time, reducing PKM2 can increase the sensitivity of tumor cells to drugs such as docetaxel and cisplatin, thereby promoting tumor tissue death and reducing tumor occurrence [32]. GLUT1 is an important carrier protein responsible for transporting glucose. The results of this study showed that after overexpressing PLCD3, the expression of glucose transporter protein GLUT1 in lung cancer cells was upregulated, increasing multiple pathways for glucose uptake and participation in sugar metabolism. In addition, the use of glycolysis inhibitors or PKC inhibitors can reduce the expression of GLUT1. The results of this study suggest that PLCD3 can cause changes in glucose metabolism in lung cancer cells and play a key role in the progression of cancer. The development of drugs targeting PLCD3 may provide effective prospects for inhibiting the occurrence and development of lung cancer and treatment.

The research additionally found that PLCD3 enhances the invasive and migratory capacities of lung cancer cells. Regarding the direct mechanism of PLCD3's impact on cell invasion, although we did not explore the specific molecular mechanisms in detail in the current study, existing literature has reported that PLCD3 may influence cell migration and invasion by regulating certain signaling pathways, such as Hippo and JAK2/STAT3 signaling pathways [9,33,34]. The Hippo signaling cascade is essential for controlling cell growth, programmed cell death, and the renewal of stem cells, whereas the JAK2/STAT3 pathway is significantly involved in cellular development, specialization, and immune system functions. Earlier research indicates that PLCD3 enhances the ability of cancer cells to migrate and invade by modulating these signaling pathways. Additionally, PLCD3 may further enhance cell invasiveness by affecting cytoskeletal reorganization and the expression of cell adhesion molecules. Future research should further validate these hypotheses to comprehensively elucidate the role of PLCD3 in tumor cell invasion and migration.

5. Conclusion

In summary, the experimental results of this study show that PLCD3 is increased in lung cancer tissues. The PLCD3 protein enhances lung cancer cell growth and metabolic changes by triggering the PKC-dependent Rap1 signaling route. The precise process involves PLCD3 triggering PKC, which subsequently stimulates the Rap1 pathway, thereby enhancing glycolysis reprogramming to supply adequate energy and metabolic materials. PLCD3 enhances the levels of GLUT1, HK1, HK2, and PKM2, thereby promoting the growth and spread of lung cancer cells. Additional experiments indicate that blocking PKC can counteract the cancer-promoting impact of PLCD3, thus reducing the growth and spread of lung cancer cells. In summary, this research uncovers how PLCD3 operates in lung cancer and offers fresh perspectives for its treatment. Inhibiting PLCD3, PKC, and the Rap1 pathway may be effective strategies for treating lung cancer. Furthermore, this research serves as a guide for exploring the role of PLCD3 in various other cancers. It is important to note that this research still has a few limitations. For instance, this research focused solely on the role of PLCD3 in lung cancer, necessitating additional studies to explore its function in other tumor types. In addition, this study needs further verification and optimization to improve the reliability and reproducibility of the research results.

Ethics approval and consent to participate

The animal experiments met the ethical requirements and were approved by the Animal Care Ethics Committee of Tianjin First Central Hospital (2022-05-A5). We confirm that all animal experiments reported in the manuscript were conducted in accordance with the ARRIVE guidelines.

Consent for publication

Not applicable.

Data availability statement

Data included in article/supp. material/referenced in article.

CRediT authorship contribution statement

Liang Zhang: Writing – review & editing, Writing – original draft, Validation, Investigation, Formal analysis, Conceptualization. **Mingjiang Li:** Formal analysis, Conceptualization. **Xiaoping Li:** Methodology, Data curation. **Ting Xiao:** Validation, Software. **Honggang Zhou:** Writing – review & editing, Investigation. **Weidong Zhang:** Writing – original draft, Project administration, Funding acquisition, Conceptualization. **Ping Wang:** Supervision, Resources, Data curation, Conceptualization.

Declaration of competing interest

The authors declare that they have no known competing financial interests or personal relationships that could have appeared to influence the work reported in this paper.

Appendix A. Supplementary data

Supplementary data to this article can be found online at https://doi.org/10.1016/j.heliyon.2024.e37063.

References

[1] R.L. Siegel, et al., Cancer statistics, CA: a cancer journal for clinicians 72 (1) (2022), 2022.
[2] H. Sung, et al., Global cancer statistics 2020: GLOBOCAN estimates of incidence and mortality worldwide for 36 cancers in 185 countries, CA: a cancer journal for clinicians 71 (3) (2021) 209–249.
[3] K. Xie, et al., BARX2/FOXA1/HK2 axis promotes lung adenocarcinoma progression and energy metabolism reprogramming, Transl. Lung Cancer Res. 11 (7) (2022) 1405.
[4] K. Eltayeb, et al., Reprogramming of lipid metabolism in lung cancer: an overview with focus on EGFR-Mutated non-small cell lung cancer, Cells 11 (3) (2022) 413.
[5] Y. Zhang, et al., Targeting glucose metabolism enzymes in cancer treatment: current and emerging strategies, Cancers 14 (19) (2022) 4568.
[6] L.M. Becker, et al., Epigenetic reprogramming of cancer-associated fibroblasts deregulates glucose metabolism and facilitates progression of breast cancer, Cell Rep. 31 (9) (2020) 107701.
[7] H. Kim, et al., Assignment (1) of the human PLC delta3 gene (PLCD3) to human chromosome band 17q21 by fluorescence in situ hybridization, Cytogenet. Genome Res. 87 (3/4) (1999) 209.
[8] W. Liu, et al., PLCD3, a flotillin2-interacting protein, is involved in proliferation, migration and invasion of nasopharyngeal carcinoma cells, Oncol. Rep. 39 (1) (2018) 45–52.
[9] L. Lin, et al., Phospholipase C Delta 3 inhibits apoptosis and promotes proliferation, migration, and invasion of thyroid cancer cells via Hippo pathway, Acta Biochim. Biophys. Sin. 53 (4) (2021) 481–491.
[10] S. He, et al., Targeting protein kinase C for cancer therapy, Cancers 14 (5) (2022) 1104.
[11] T. Kawano, et al., Activators and inhibitors of protein kinase C (PKC): their applications in clinical trials, Pharmaceutics 13 (11) (2021) 1748.
[12] X. Su, et al., SGSM2 inhibits thyroid cancer progression by activating RAP1 and enhancing competitive RAS inhibition, Cell Death Dis. 13 (3) (2022) 218.
[13] E. Khattar, V. Tergaonkar, Role of Rap1 in DNA damage response: implications in stem cell homeostasis and cancer, Exp. Hematol. 90 (2020) 12–17.
[14] E. Khattar, et al., Rap1 regulates hematopoietic stem cell survival and affects oncogenesis and response to chemotherapy, Nat. Commun. 10 (1) (2019) 5349.
[15] R.V. Pusapati, et al., mTORC1-dependent metabolic reprogramming underlies escape from glycolysis addiction in cancer cells, Cancer Cell 29 (4) (2016) 548–562.
[16] R.J. DeBerardinis, N.S. Chandel, We need to talk about the Warburg effect, Nat. Metab. 2 (2) (2020) 127–129.
[17] B. Zhou, S. Zong, W. Zhong, et al., Interaction between laminin-5γ2 and integrin β1 promotes the tumor budding of colorectal cancer via the activation of Yes-associated proteins, Oncogene 39 (7) (2020) 1527–1542.
[18] P. Vaupel, G. Multhoff, Revisiting the Warburg effect: historical dogma versus current understanding, J. Physiol. 599 (6) (2021) 1745–1757.
[19] W. Zhong, et al., Cartilage oligomeric matrix protein promotes epithelial-mesenchymal transition by interacting with transgelin in colorectal cancer, Theranostics 10 (19) (2020) 8790.
[20] B. Ruprecht, et al., Lapatinib resistance in breast cancer cells is accompanied by phosphorylation-mediated reprogramming of glycolysis, Cancer Res. 77 (8) (2017) 1842–1853.

[21] Y. Tan, et al., Metabolic reprogramming from glycolysis to fatty acid uptake and beta-oxidation in platinum-resistant cancer cells, Nat. Commun. 13 (1) (2022) 4554.

[22] J. Koivunen, V. Aaltonen, J. Peltonen, Protein kinase C (PKC) family in cancer progression, Cancer Lett. 235 (1) (2006) 1–10.

[23] G. Martiny-Baron, D. Fabbro, Classical PKC isoforms in cancer, Pharmacol. Res. 55 (6) (2007) 477–486.

[24] G.C. Blobe, L.M. Obeid, Y.A. Hannun, Regulation of protein kinase C and role in cancer biology, Cancer Metastasis Rev. 13 (1994) 411–431.

[25] A.C. Kimmelman, Metabolic dependencies in RAS-driven cancers, Clin. Cancer Res. 21 (8) (2015) 1828–1834.

[26] H. Ying, et al., Oncogenic Kras maintains pancreatic tumors through regulation of anabolic glucose metabolism, Cell 149 (3) (2012) 656–670.

[27] E.M. Kerr, et al., Mutant Kras copy number defines metabolic reprogramming and therapeutic susceptibilities, Nature 531 (7592) (2016) 110–113.

[28] W.G. Kaelin Jr, C.B. Thompson, Clues from cell metabolism, Nature 465 (7298) (2010) 562–564.

[29] W.H. Koppenol, P.L. Bounds, C.V. Dang, Otto Warburg's contributions to current concepts of cancer metabolism, Nat. Rev. Cancer 11 (5) (2011) 325–337.

[30] S.N. Garcia, R.C. Guedes, M.M. Marques, Unlocking the potential of HK2 in cancer metabolism and therapeutics, Curr. Med. Chem. 26 (41) (2019) 7285–7322.

[31] Z. Zhang, et al., PKM2, function and expression and regulation, Cell Biosci. 9 (2019) 1–25.

[32] K. Zahra, et al., Pyruvate kinase M2 and cancer: the role of PKM2 in promoting tumorigenesis, Front. Oncol. 10 (2020) 159.

[33] M. Wang, et al., PLCD3 promotes malignant cell behaviors in esophageal squamous cell carcinoma via the PI3K/AKT/P21 signaling, BMC Cancer 23 (1) (2023) 921.

[34] Y. Yu, et al., PLCD3 inhibits apoptosis and promotes proliferation, invasion and migration in gastric cancer, Discover Oncology 15 (1) (2024) 26.